https://doi.org/10.5194/egusphere-2023-22
Preprint. Discussion started: 11 January 2023

The Influence of Carbon Cycling on Oxygen Depletion in North-Temperate Lakes

Austin Delany[1], Robert Ladwig[1], Cal Buelo[1], Ellen Albright[1], Paul C. Hanson[1]
[1] Center for Limnology, University of Wisconsin-Madison, Madison, WI, USA
Correspondence to: Austin Delany (addelany@wisc.edu)

Abstract. Hypolimnetic oxygen depletion during summer stratification in lakes can lead to hypoxic and anoxic conditions. Hypolimnetic anoxia is a water quality issue with many consequences, including reduced habitat for cold-water fish species, reduced quality of drinking water, and increased nutrient and organic carbon (OC) release from sediments. Both allochthonous and autochthonous OC loads contribute to oxygen depletion by providing substrate for microbial respiration; however, their relative importance in depleting oxygen across diverse lake systems remains uncertain. Lake characteristics, such as trophic state, hydrology, and morphometry are also influential in carbon cycling processes and may impact oxygen depletion dynamics. To investigate the effects of carbon cycling on hypolimnetic oxygen depletion, we used a two-layer process-based lake model to simulate daily metabolism dynamics for six Wisconsin lakes over twenty years (1995-2014). Physical processes and internal metabolic processes were included in the model and were used to predict dissolved oxygen (DO), particulate OC (POC), and dissolved OC (DOC). In our study of oligotrophic, mesotrophic, and eutrophic lakes, we found autochthony to be far more important than allochthony to hypolimnetic oxygen depletion. Autochthonous POC respiration in the water column contributed the most towards hypolimnetic oxygen depletion in the eutrophic study lakes. POC water column respiration and sediment respiration had similar contributions in the mesotrophic and oligotrophic study lakes. Differences in source

https://doi.org/10.5194/egusphere-2023-22
Preprint. Discussion started: 11 January 2023

of respiration are discussed with consideration of lake productivity, hydrology, and morphometry.

https://doi.org/10.5194/egusphere-2023-22
Preprint. Discussion started: 11 January 2023

1 Introduction

Hypolimnetic oxygen depletion impacts lake ecosystems through its influences on lake habitat and organic carbon (OC) cycling (Cole & Weihe 2016). In many lakes, oxygen depletion results in hypoxia and even anoxia (Nürnberg 1995). Hypolimnetic anoxia reduces habitat availability for cold-water fish species (Magee et al. 2019), reduces quality of drinking water (Bryant et al. 2011), and can lead to elevated nutrient and OC release from lake sediments (Hoffman et al. 2013, McClure et al. 2020). The formation of hypolimnetic anoxia is associated with many internal and external lake characteristics, such as trophic status (Rhodes et al., 2017; Rippey & McSorley, 2009), lake morphometry (Livingstone & Imboden, 1996), and hydrology (Nürnberg 2004). An increase in the prevalence of hypolimnetic anoxia and associated water quality degradation in temperate lakes indicates the need to better understand how lake ecological processes interact with external forcing to lead to the development of anoxia (Jane et al. 2021).

Hypolimnetic anoxia can occur when water column and sediment microbial respiration rates exceed rates of oxygenation over an extended period. The conditions supporting oxygen depletion are the outcomes of complex ecosystem processes and the interactions of the lake with its climate and landscape settings (Jenny et al. 2016a, 2016b). Autochthonous OC inputs vary considerably across trophic gradients and are a labile substrate for microbial respiration that can contribute substantially to hypolimnetic anoxia (Müller et al. 2012, 2019). Allochthonous OC sources have also been shown to impact dissolved oxygen (DO) and carbon dynamics in lakes by providing a more consistent and recalcitrant substrate for

https://doi.org/10.5194/egusphere-2023-22
Preprint. Discussion started: 11 January 2023

respiration (Hanson et al. 2014, Solomon et al. 2015). Non-biological factors can be important as well, such as the watershed loading of allochthonous OC, which can influence the overall lability of OC in a lake and the rate of DO depletion (Hotchkiss et al. 2018). Physical factors, such as stratification onset, water column stability, and vertical mixing, can control the transport of DO from oxygen-rich upper layers to the lower layers of a lake, and can therefore limit oxygen availability in the hypolimnion (Snortheim et al. 2017, Ladwig et al. 2021). Lake morphometry can influence the spatial extents of stratified layers, which can have profound effects on hypolimnetic volume and its capacity to hold DO as well as the rate of sediment oxygen consumption, which can both influence anoxia onset in lakes (Livingstone & Imboden 1996). Thus, the sources and lability of OC, lake morphometry, and lake hydrodynamics all contribute to hypolimnetic oxygen depletion rates, making it an emergent ecosystem property with a plethora of causal relationships to other ecologically important variables.

Although previous studies have investigated contributions of allochthonous and autochthonous OC to lake carbon cycling (Hanson et al. 2014, McCullough et al. 2018), the effects on formation of hypolimnetic anoxia deserves further exploration (Hanson et al. 2015). The magnitude and relative balance of the sources of OC loads relates to hypolimnetic anoxia across trophic and hydrology gradients (Rhodes et al., 2017; Rippey and McSorley, 2009, Hanson et al. 2014). These gradients affect the relative contributions of autochthony and allochthony in a lake, which further control the lability and fates (respiration, burial, export) of OC. The lability of OC relates to its form and its source (Hotchkiss et al. 2018,

https://doi.org/10.5194/egusphere-2023-22
Preprint. Discussion started: 11 January 2023

Catalán et al. 2016). Autochthonous POC and DOC tend to be much more labile than allochthonous OC (Amon & Brenner 1996, Thorpe & Delong 2002), thus understanding both the forms of OC and their origins, in addition to their magnitudes, informs our understanding of the controls over lake respiration. Quantifying the contribution of these different factors to hypolimnetic anoxia is crucial to understanding its drivers across lakes and through time.

The availability of long-term observational data combined with process-based models provides an opportunity to investigate OC sources and their control over the dynamics of lake DO across multiple time scales. Long-term studies of lakes on regional and global scales highlight how environmental trends can influence metabolic processes in lakes, and how lakes can broaden our understanding of large-scale ecosystem processes (Richardson et al. 2017, Kraemer et al. 2017, Williamson et al. 2008). For example, long-term studies allow us to investigate the impact that current and legacy conditions have on lake ecosystem function in a given year (Carpenter et al. 2007). Process-based modeling has been used to investigate metabolism dynamics and understand both lake carbon cycling (Hanson et al. 2004, Cardille et al. 2007) and formation of anoxia (Ladwig et al. 2022); however, explicitly tying lake carbon cycling and metabolism dynamics with long-term hypolimnetic DO depletion across a variety of lakes remains largely unexplored. The combination of process-based modeling with available long-term observational data, including exogenous driving data representative of climate variability, can be especially powerful for recreating representations of long-term lake metabolism dynamics (Staehr et al. 2010, Cardille et al. 2007).

https://doi.org/10.5194/egusphere-2023-22
Preprint. Discussion started: 11 January 2023

In this study, our goal is to investigate OC source contributions to lake carbon cycling and hypolimnetic oxygen depletion. We are particularly interested in the relative loads of autochthonous and allochthonous OC to lakes and how they contribute to hypolimnetic DO depletion across seasonal to decadal scales. We use a process-based lake metabolism model, combined with daily external driving data and long-term limnological data, to study six lakes within the North Temperate Lakes Long-Term Ecological Research network (NTL LTER) over a twenty-year period (1995-2014). We address the following questions: (1) What are the dominant sources of organic carbon that contribute to hypolimnetic oxygen depletion, and how do their contributions differ across a group of diverse lakes over two decades? (2) How do lake trophic state, hydrology, and morphometry influence the processing and fates of organic carbon loads in ways that affect hypolimnetic dissolved oxygen?

2 Methods

2.1 Study Site

This study includes six Wisconsin lakes from the NTL-LTER program (Magnuson et al. 2006). Trout Lake (TR), Big Muskellunge Lake (BM), Sparkling Lake (SP), and Allequash Lake (AL) are in the Northern Highlands Lake District of Wisconsin and have been regularly sampled since 1981 (Magnuson et al. 2006). Lake Mendota (ME) and Lake Monona (MO) are in southern Wisconsin and have been regularly sampled by the NTL-LTER since 1995 (NTL-LTER, Magnuson et al. 2006). The NTL-LTER provides a detailed description of each lake (Magnuson et al. 2006). The six lakes span gradients in size, morphometry, landscape setting, and hydrology, which creates diverse carbon cycling characteristics and processes

https://doi.org/10.5194/egusphere-2023-22
Preprint. Discussion started: 11 January 2023

156 across these systems. TR and AL are drainage lakes with high allochthonous carbon inputs
157 from surface water, while BM and SP are groundwater seepage systems with allochthony
158 dominated by aerial OC inputs from the surrounding landscape (Hanson et al. 2014). All four
159 northern lakes (TR, AL, BM, SP) are surrounded by a forested landscape. ME and MO are
160 both eutrophic drainage lakes surrounded by an urban and agricultural landscape.
161 Morphometry, hydrology, and other information can be found in Table 1.

162
163 **Table 1.** Physical and biogeochemical characteristics of the study lakes. The table includes
164 lake area (Area), maximum depth (Zmax), hydrologic residence time (RT), mean annual
165 temperature (Temp), mean annual surface total phosphorus concentration (Mean TP), and
166 mean annual surface DOC (Mean DOC).
167

Lake	Area (ha)	Zmax (m)	RT [3,4] (years)	Temp [2] (°C)	Mean TP [1] (µgL)	Mean DOC [1] (mgL)
Allequash Lake (AL)	168.4	8	0.73	10.5	14	3.9
Big Muskellunge (BM)	396.3	21.3	5.1	10.5	7	3.8
Sparkling Lake (SP)	64	20	8.88	10.6	5	3.12
Trout Lake (TR)	1607.9	35.7	5.28	9.8	5	2.8
Mendota (ME)	3961	25.3	4.3	12.5	50	5.6
Monona (MO)	1324	22.5	0.7	13.8	47	5.8

168
169 1 - Magnuson et al. (2020, 2006)
170 2 - Magnuson et al. (2022)

https://doi.org/10.5194/egusphere-2023-22
Preprint. Discussion started: 11 January 2023

3 - Hunt et al. (2013)
4 - Webster et al. (1996)

2.2 Driving Data and Limnological Data

Most driving data for the model is provided by the "Process-based predictions of water temperature in the Midwest US" USGS data product (Read et al. 2021). This includes lake characteristic information such as lake area and hypsometry, daily modeled temperature profiles, ice flags, meteorology data, and solar radiation for the six study lakes. Derived hydrology data is used in calculating daily OC loading and outflow for the study lakes. Hydrology for the northern lakes is taken from Hunt & Walker (2017), which was estimated using a surface and groundwater hydrodynamic model. Hydrology for ME is taken from Hanson et al. (2020), which used the Penn State Integrated Hydrologic Model (Qu & Duffy 2007). We found that the derived discharge data for ME, TR, AL, and SP was approximately 20-50% higher than previously reported values (Hunt et al. 2013, Webster et al. 1996), depending on the lake, while hydrology in BM was approximately 25% too low (Hunt et al. 2013). To accommodate this issue, we adjusted total annual hydrological inputs to match published water residence times for each lake (Table 1), while retaining temporal hydrological patterns. NTL-LTER observational data are interpolated to estimate daily nutrient concentration values, which are used in calculating daily primary production in the model (Magnuson et al. 2020).

https://doi.org/10.5194/egusphere-2023-22
Preprint. Discussion started: 11 January 2023

The NTL-LTER observational data used to calibrate and validate the model for the six lakes include DO, DOC, and Secchi depth (Magnuson et al. 2020, Magnuson et al. 2022). Saturation values for DO and gas exchange velocity used in calculating atmospheric exchange for DO are calculated using the "o2.at.sat.base" and using the Cole and Caraco gas exchange method from the "K600.2.KGAS.base" function within the USGS "LakeMetabolizer" package in R (Winslow et al. 2016).

2.3 The Model

The goal of our model is to use important physical and metabolic processes involved in the lake ecosystem carbon cycle to best predict DO, DOC, and POC, while keeping the model design simple in comparison with more comprehensive water quality models (e.g., Hipsey et al. 2019). We ran our model with a daily time step over a twenty-year period for each lake and includes seasonal physical dynamics, such as lake mixing, stratification, and ice cover from Read et al. 2021. Throughout each year, the model tracks state variables and fluxes in the lake for each day (Fig. 1). These state variables include DO and the labile and recalcitrant components of particulate organic carbon (POC) and dissolved organic carbon (DOC). During stratified periods, the state variables and fluxes for the epilimnion and hypolimnion are tracked independently. Atmosphere, sediments, and hydrologic inputs and outputs are boundary conditions.

https://doi.org/10.5194/egusphere-2023-22
Preprint. Discussion started: 11 January 2023

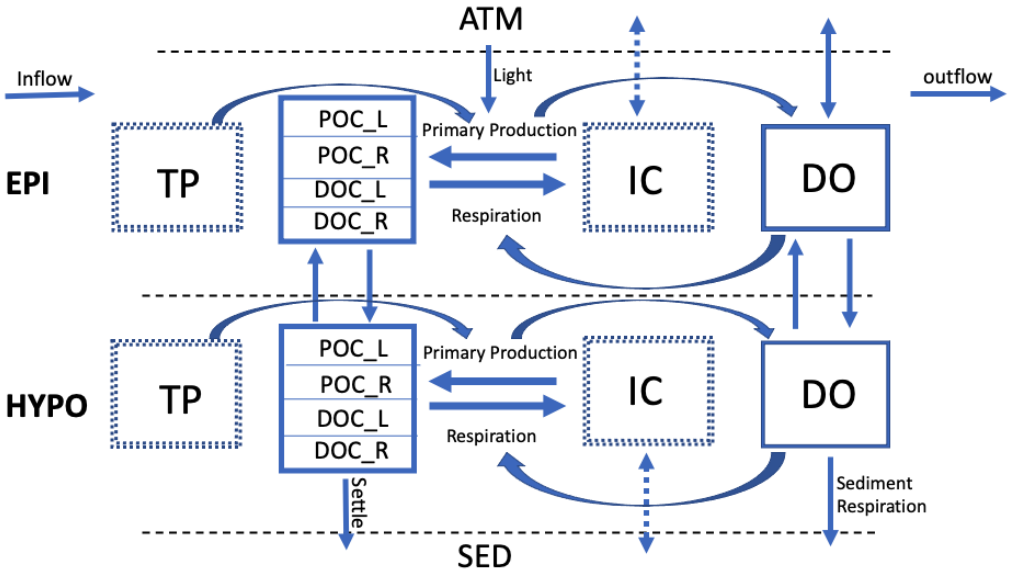

Figure 1. Conceptual lake model showing state variables (boxes) and fluxes (arrows). The model has two thermal layers under stratified conditions, as shown here, and tracks state variables separately for each layer. The sediment (SED), atmosphere (ATM), inflow and outflow are system boundaries. The state variables included are DO (dissolved oxygen), DOC_L (labile dissolved organic carbon), DOC_R (recalcitrant dissolved organic carbon), POC_L (labile particulate organic carbon), and POC_R (recalcitrant particulate organic carbon). Inorganic carbon (IC) is not tracked in the model and is assumed to be a non-limiting substrate to primary production. Observed total phosphorus (TP) is used as a driving variable for primary production in the model.

2.3.1 Stratification Dynamics

Lake physical dynamics are taken from the output of a previous hydrodynamic modeling study on these same lakes over a similar time period (Read et al. 2021), which used the General Lake Model (Hipsey et al. 2019). Before running the metabolism model, a thermocline depth for each time step is estimated using derived temperature profiles for each lake (Read et al. 2021) by determining the center of buoyancy depth (Read et al. 2011). After calculating the thermocline depth, the volumes and average temperatures for each layer, and the specific area at thermocline depth are determined using lake-specific hypsography. The

https://doi.org/10.5194/egusphere-2023-22
Preprint. Discussion started: 11 January 2023

criteria for stratification include a vertical density gradient between the surface and bottom layer of at least 0.05 kg m^{-3}, an average water column temperature above 4 °C, and the presence of a derived thermocline (Ladwig et al. 2022). For any day that does not meet all of these criteria, the water column is considered to be fully mixed. The thermocline depth values are smoothed using a moving average with a window size of 14 days to prevent large entrainment fluxes that can destabilize the model at very short time scales when thermal strata are shallow. During mixed periods, the entire lake is treated as the epilimnion, and a separate hypolimnion is not incorporated into the model dynamics. Ice cover in the model is determined using the "ice flag" provided in the derived temperature profile data from Read et al. (2021). Our metabolism model does simulate under-ice conditions, however we do not include the presence of inverse stratification during winter periods.

2.3.2 External Lake and Environment Physical Fluxes

Atmospheric exchange of DO, external loading of OC, and outflow of OC are the three environmental boundary fluxes accounted for in the water quality model (Table 3 Eq. 9-11). The gas exchange velocity for atmospheric exchange is determined using the Cole and Caraco model (1998) and is calculated using the LakeMetabolizer R package (Winslow et al. 2016). Oxygen saturation values are also calculated using this package. During ice covered conditions, we assume that the atmospheric exchange value is ten percent of the value during non-ice covered conditions based on sea ice gas exchange estimates (Loose and Schlosser, 2011).

https://doi.org/10.5194/egusphere-2023-22
Preprint. Discussion started: 11 January 2023

For the northern lakes (TR, AL, BM, SP), we use the allochthonous OC load and recalcitrant OC export values from Hanson et al. (2014) to calibrate total annual allochthonous OC load and recalcitrant OC export in our model. We specifically use the allochthonous OC load values in this study to assist in the manual calibration of inflow recalcitrant POC and DOC concentrations for each lake. For the southern lakes (ME, MO), we also use derived hydrology information (Hanson et al. 2020), but only for discharge that is the inflow for ME. We assume for ME and MO that evaporation from the lake surface is approximately equal to precipitation on the lake surface and that groundwater inputs and outputs to the lake are a small part of the hydrologic budgets (Lathrop & Carpenter 2014). Therefore, ME outflow is assumed to be equal to ME inflow. ME is the predominant hydrologic source for MO (Lathrop & Carpenter 2014), thus, MO inflow is assumed to be equal to ME outflow, and MO outflow is assumed to be equal to MO inflow. ME allochthonous load is calibrated based on model fitting and observational data (Hart et al. 2019). MO inflow concentrations are equivalent to the in-lake epilimnetic concentrations of OC from ME at each model time step. The OC loads for MO are calibrated based on the total allochthonous load found in McCullough et al. 2018.

Table 2. Equations for the model, organized by state variables, [*DO* (dissolved oxygen), *DOC_L* (labile dissolved organic carbon), *DOC_R*(recalcitrant dissolved organic carbon), *POC_L* (labile particulate organic carbon), *POC_R* (recalcitrant particulate organic carbon), *Secchi*] and relevant fluxes. *Note:* The entrainment flux (*Entr*) is only included during thermally stratified periods. The inflow (*IN*) and outflow (*OUT*) fluxes are not included in the calculations for the hypolimnetic layer. Atmospheric gas exchange of dissolved oxygen (*AtmExch*) is not included for the hypolimnetic DO calculation. Normalized total phosphorus is represented by (TP_{norm}). The volume (*V*) term represents the respective lake layer volume,

https://doi.org/10.5194/egusphere-2023-22
Preprint. Discussion started: 11 January 2023

282 or the discharge volume for the inflow and outflow equations. Terms not defined here are
283 included in Table 3.
284

State Variables	
DO [gDO] $\frac{dDO}{dt} = NPP * O2_{convert}) + AtmExch + Entr_{DO} - (R_{sed} * O2_{convert}) - (R_{wc} * O2_{convert})$	(1)
DOC_L [gC] $\frac{dDOC_L}{dt} = (NPP * (1 - C_{NPP})) + IN_{DOCL} + Entr_{DOCL} - R_{DOCL} - OUT_{DOCL}$	(2)
DOC_R [gC] $\frac{dDOC_R}{dt} = IN_{DOCR} + Entr_{DOCR} - OUT_{DOCR} - R_{DOCR\,Epi}$	(3)
POC_L [gC] **Mixed and Epi:** $\frac{dPOC_L}{dt} = (NPP_{Epi} * C_{NPP}) + IN_{POCL} + Entr_{POCL} - R_{POCL\,Epi} - Settle_{POCL\,Epi} - OUT_{POCL}$ **Hypo:** $\frac{dPOC_L}{dt} = (NPP_{Hypo} * C_{NPP}) + Settle_{POCL\,Epi} - Settle_{POCL\,Hypo} - R_{POCL\,Hypo} - Ent_{POCL}$	(4) (5)
POC_R [gC] **Mixed and Epi:** $\frac{dPOC_R}{dt} = IN_{POCR} + Entr_{POCR} - OUT_{POCR} - R_{POCR\,Epi} - Settle_{POCR\,Epi}$ **Hypo:** $\frac{dPOC_R}{dt} = Settle_{POCR\,Epi} - Settle_{POCR\,Hypo} - R_{POCR\,Hypo} - Entr_{POCR}$	(6) (7)
Secchi [m] $Secchi = \frac{1.7}{K_{LEC}}$	(8)
Fluxes	
Atm exchange [gDO d^{-1}] $AtmExch = K_{DO} * (DO_{sat} - DO_{prediction}) * Area_{sfc}$	(9)
Inflow [gC d^{-1}] $IN = Carbon\ Concentration_{inflow} * V_{inflow}$	(10)
Outflow [gC d^{-1}] $OUT = Carbon\ Concentration_{outflow} * V_{outflow}$	(11)
Net Primary Productivity [gC d^{-1}] $NPP = Pmax * (1 - e^{(-IP * \frac{Light}{Pmax})}) * TP_{norm} * \theta_{NPP}{}^{(T-20)} * V$	(12)
Respiration [gC d^{-1}] $R = Carbon\ Pool * r_{rate} * \theta_{Resp}{}^{(T-20)} * \frac{DO\ Concentration}{DO_{1/2} + DO\ Concentration}$	(13)
Sediment Respiration [gC d^{-1}] $R_{sed} = r_{sed} * \theta_{Resp}{}^{(T-20)} * \frac{DO\ Concentration}{DO_{1/2} + DO\ Concentration} * Area_{sed}$	(14)
POC settle [gC d^{-1}] $Settle = (POC\ Pool * K_{POC}) * \frac{Area}{V}$	(15)
Entrainment [gC d^{-1}] $V_{Entr} = V_{epi}(t) - V_{epi}(t-1)$	(16)
$V_{Entr} > 0$ (Epilimnion growing) $Entr = \frac{V_{Entr}}{V_{Hypo}} * Carbon\ Pool_{Hypo}$	(17)
$V_{Entr} < 0$ (Epilimnion shrinking) $Entr = \frac{V_{Entr}}{V_{Epi}} * Carbon\ Pool_{Epi}$	(18)

https://doi.org/10.5194/egusphere-2023-22
Preprint. Discussion started: 11 January 2023

Light [W m^{-2}] $Light = \int_{z_1}^{z_2}(I_{z_1} * e^{-(K_{LEC} * z)})\, dz * (1 - \alpha)$	(19)
Light Extinction Coefficient [Unitless] $K_{LEC} = LEC_{water} + (LEC_{POC} * ((\frac{POCL}{V}) + (\frac{POCR}{V}))) + (LEC_{DOC} * ((\frac{DOCL}{V}) + (\frac{DOCR}{V})))$	(20)

2.3.3 Internal Lake Physical Fluxes

The two in-lake physical fluxes included in the model are POC settling and entrainment of all state variables. POC settling is the product of a sinking rate (m d^{-1}) and the respective POC pool (g), divided by the layer depth (m) (Table 3 Eq. 15). Sinking rates are either borrowed from literature values (Table 3) or fit during model calibration (see below). Entrainment is calculated as a proportion of epilimnetic volume change (Table 2 Eq. 17-18). A decrease in epilimnetic volume shifts mass of state variables from the epilimnion into the hypolimnion, and an increase in volume shifts mass from the hypolimnion to the epilimnion.

Table 3. Model Parameters, grouped by static and free parameters

Parameter	Abbreviation	Value	Units	Comments
Respiration rate of DOCR	r_{DOCR}	0.001	day^{-1}	(Hanson et al., 2011)
Respiration rate of POCR	r_{POCR}	0.005	day^{-1}	Based on ranges provided in (Hanson et al. 2004) and estimated from manual model fitting
Respiration rate of POCL	r_{POCL}	0.2	day^{-1}	Based on ranges provided in (Hipsey et al. 2019) and estimated from manual model fitting
Michaelis-Menten DO half saturation coefficient	$DO_{1/2}$	0.5	$g\ \ m^{-3}$	Determined through manual model fitting
Conversion of Carbon to Oxygen	$O2_{convert}$	2.67	Unitless	Mass Ratio of C:O
Fitting coefficient for Light extinction of water	LEC_{water}	0.125	m^{-1}	Manually calibrated based on observed Secchi Depth ranges for the study lakes
Fitting coefficient for Light extinction of DOC	LEC_{DOC}	0.02 - 0.06	$m^2 g^{-1}$	Manually calibrated based on observed Secchi Depth ranges for the study lakes

https://doi.org/10.5194/egusphere-2023-22
Preprint. Discussion started: 11 January 2023

Fitting coefficient for Light extinction of POC	LEC_{POC}	0.7	$m^2 g^{-1}$	Manually calibrated based on observed Secchi Depth ranges for the study lakes
Ratio of DOC to POC production from NPP	C_{NPP}	0.8	Unitless	Hipsey et al. 2019 Hipsey et al. 2019
Atmospheric gas exchange adjustment during ice covered conditions	C_{winter}	0.1	Unitless	Estimated from manual model fitting and ranges provided in (Loose & Schlosser, 2011)
Coefficient of light transmitted through ice	C_{ice}	0.05	Unitless	Based on ranges provided in (Lei et al. 2011) and estimated from manual model fitting
Settling velocity rate of POC_R	K_{POCR}	1.2	$m\ \ day^{-1}$	Based on ranges found in (Reynolds et al.1987) and estimated from manual model fitting
Settling velocity rate of POC_L	K_{POCL}	1	$m\ \ day^{-1}$	Based on ranges ranges found in (Reynolds et al.1987) and estimated from manual model fitting
Temperature scaling coefficient for NPP	θ_{NPP}	1.12	Unitless	Based on Q10 of 2 principles and estimated from manual model fitting
Temperature scaling coefficient for Respiration	θ_{Resp}	1.04	Unitless	Based on Q10 of 2 principle and estimated from manual model fitting
Albedo	α	0.3	Unitless	Global average (Marshall & Plumb, 2008)
Maximum Daily Productivity	$Pmax$	0.5-5	$g\ \ m^{-3} day^{-1}$	Range based on mean productivity values from Wetzel (2001) and manual model fitting
Recalcitrant DOC inflow concentration	$DOCR_{inflow}$	5-10	$g\ \ m^{-3}$	Based on ranges found in (Hanson et al. 2014, McCullough et al. 2018, Hart et al. 2017) and manual model fitting
Recalcitrant POC inflow concentration	$POCR_{inflow}$	2-5	$g\ \ m^{-3}$	Based on ranges found in (Hanson et al. 2014, McCullough et al. 2018, Hart et al. 2017) and manual model fitting
Free parameters				
Slope of the irradiance/productivity curve	IP	0.055, 0.020	$gCd^{-1}(Wm^{-2})^{-1}$	Based on ranges found in (Platt et al. 1980) and fit for each lake region independently (South, North)
Respiration rate of sediments	r_{sed}	0.1 – 0.4	day^{-1}	Fit independently for each lake
Respiration rate of DOCL	r_{DOCL}	0.015, 0.020	day^{-1}	Fit for each lake region independently (South, North)

https://doi.org/10.5194/egusphere-2023-22
Preprint. Discussion started: 11 January 2023

298

299 **2.3.4 Internal Lake Metabolism Fluxes**

300 The metabolism fluxes in the model are net primary production (NPP) and respiration (R).
301 Respiration includes water column respiration for each OC state variable in the epilimnion
302 and hypolimnion and is calculated at each time step as the product of the OC state variable
303 and its associated first order decay rate (Table 2, Eq. 13). Sediment respiration for the
304 hypolimnion during stratified periods and the epilimnion (entire lake) during mixed periods
305 is a constant daily rate that is individually fit for each lake. We assume inorganic carbon is
306 not a limiting carbon source. In the model, we consider any DO concentration less than 1 g
307 DO m^{-3} to be anoxic (Nürnberg 1995).

308

309 NPP is tracked in both the epilimnion and hypolimnion. NPP is a function of light, total
310 phosphorus concentration, temperature, a maximum productivity coefficient, and a slope
311 parameter defining the irradiance and productivity curve (Table 2 Eq. 12). Average light in a
312 layer is calculated for each day and is dependent on the depth of a layer and the light
313 extinction coefficient (Table 2 Eq. 19). During ice covered conditions, average light is
314 assumed to be five percent of the average non-ice covered value (Lei et al. 2011). Total
315 phosphorus concentration in a layer is from observational data for each lake interpolated to
316 the daily time scale. The interpolated values are then normalized for each individual lake to
317 drive NPP. These values are normalized so that differences among lakes are only present in
318 the IP and P_{max} parameters. The Arrhenius equation provides temperature control for NPP,
319 and we determined through model fitting a θ of 1.12. OC derived from NPP is split between

https://doi.org/10.5194/egusphere-2023-22
Preprint. Discussion started: 11 January 2023

particulate and dissolved labile OC production, with eighty percent produced as POC and twenty percent produced as DOC. This ratio was determined through model fitting and is similar to previously reported values (Hipsey et al. 2019).

Epilimnetic and hypolimnetic water column respiration is tracked independently for each OC pool in the model. During mixed periods, there are four OC pools – DOCR, DOCL, POCR, POCL. During stratified periods, those pools are split into a total of eight pools that are tracked independently for the epilimnion and hypolimnion. Respiration is calculated as a product of the mass of a respective variable, a first order decay rate coefficient, temperature, and oxygen availability (Table 2 Eq. 13). The respiration decay rate coefficients are based on literature values (Table 3) or were fit during model calibration. An Arrhenius equation is used for temperature control of respiration, with θ equal to 1.04, which was determined through manual model fitting. The respiration rates are also scaled by oxygen availability using the Michaelis-Menten equation with a half saturation coefficient of 0.5 g DO m^{-3}, such that at very low DO concentrations, the respiration flux approaches zero.

Sediment respiration is calculated from a constant daily respiration rate coefficient, adjusted for temperature and oxygen availability, using the Arrhenius and Michaelis-Menten equations, respectively (Table 2 Eq. 14). The mass of sediment OC is not tracked in the model. During stratified periods, we assume that the majority of epilimnetic sediment area is in the photic zone, and therefore has associated productivity from macrophytes and other biomass. It is assumed that this background productivity and sediment respiration are of

https://doi.org/10.5194/egusphere-2023-22
Preprint. Discussion started: 11 January 2023

similar magnitude and inseparable from water column metabolism, given the observational data. Therefore, epilimnetic sediment respiration is not accounted for in the model during stratified conditions. During mixed conditions, we assume that sediment respiration is active on all lake sediment surfaces, which are assumed to be equivalent in area to the total surface lake area. During stratified periods, we use the area at the thermocline as the sediment area for calculating hypolimnetic sediment respiration.

2.3.5 Other in-lake calculations and assumptions

We calculate a total light extinction coefficient (LEC) for the epilimnion and hypolimnion. The total LEC for each layer is calculated by multiplying the dissolved and particulate specific LEC values with their respective OC state variable concentrations, combined with a general LEC value for water (Table 2 Eq. 20). This total LEC value is used to calculate a daily estimate of Secchi depth (Table 2 Eq. 8). The coefficients for the light extinction of water, DOC, and POC are manually calibrated based on observed Secchi depth ranges for the study lakes (Table 3, SI Table 5).

2.4 Model calibration and validation

The model was run for twenty years from 1 January 1995 to 31 December 2014. This period was chosen due to an absence of hydrologic data for the northern lakes after 2014 and because consistent observational data weren't available for the southern lakes until 1995. The first 15 years of the model output was used for calibration and the last 5 years were used for model validation. We chose the first 15 years for calibration because the observational data

https://doi.org/10.5194/egusphere-2023-22
Preprint. Discussion started: 11 January 2023

were relatively stable and were not indicative of any large trends in ecosystem processes, as opposed to the last five years which showed slightly more model deviation from DOC observational data in the southern lakes (SI Fig. 2).

Initial conditions for each lake state variable are based on literature values or lake observational data (SI Table 5). The model is initialized on January 1st of the first year, so we set the initial labile POC mass to zero under the assumption that the concentration is low in the middle of winter. The initial DO value is set to the saturation value based on the conditions of the initial model run day and is calculated using the LakeMetabolizer R package (Winslow et al. 2016).

2.5 Model Fitting and Parameter Uncertainty Estimation

The free parameters in the model are the slope of the irradiance/productivity curve (IP), the respiration rate of labile DOC (Resp_DOCL), and the respiration rate of the hypolimnetic sediments (Resp_sed) (Table 3). These were in part chosen due to the high uncertainty around the parameter values, and our assumptions that they have a higher impact on ecosystem dynamics in the model. Optimized values and uncertainties for each free parameter and lake are included in SI Table 4.

IP controls the amount of productivity in low light scenarios, and fitting the parameter helps to calibrate productivity during ice-covered winter conditions as well as during times of high OC concentrations in the epilimnion. Resp_DOCL controls the seasonal dynamics of DOC in

https://doi.org/10.5194/egusphere-2023-22
Preprint. Discussion started: 11 January 2023

a lake and treating it as a free parameter helps capture the across-lake variability in DOC processes related to variations in landscape, hydrology, and productivity. Resp_sed is important for controlling hypolimnetic oxygen depletion in lakes and is related to lake productivity and associated legacy OC in each lake. The Resp_sed parameter also helps adjust burial rates for the study lakes. We fit unique IP and Resp_DOCL values for the southern lake region (ME, MO), and unique values for the northern region (TR, AL, BM, SP). Resp_sed is individually fit for each lake.

We manually optimized free parameters by manually adjusting them over their respective ranges to find the parameter values that returned the smallest model residuals (SI Table 4). Automated optimization proved too computationally demanding. To gain a better sense of the contributions of parameter uncertainty in the model, we created parameter uncertainty distributions using standard deviations of 20% of the estimated parameter value. To evaluate the influence of parameter uncertainties on model predictions, the parameter distributions are randomly sampled over 100 model iterations to create the uncertainty bounds for all predictions of model state variables and fluxes.

During the model fitting, errors in modeled DO, DOC, and Secchi depth are weighted equally in the southern lakes. In the northern lakes, fitting Secchi depth was challenging. Initial model fits revealed that patterns in observed Secchi did not show regular seasonality and were highly stochastic. Therefore, we use a moving average on observational data and predictions of Secchi depth and calculate the residuals as the difference between the two

https://doi.org/10.5194/egusphere-2023-22
Preprint. Discussion started: 11 January 2023

averaged time series. This is done to remove stochasticity from the observational data and fit the model predictions to the average observed Secchi value. We use a moving average window of 15 observations because we want to capture the average annual Secchi depth trend, and there are roughly 15 observations per year.

3 Results

3.1 Model Fit to Ecosystem States

Model predictions of DO reproduce observed seasonal variability well. RMSE values presented here represent model error combined over both the validation and calibration periods (see Supplementary Material: Table S1 for calibration and validation specific RMSE values). State variables are presented with truncated time ranges for visual clarity (see Supplementary Material: Fig. S1-S3 for full time series). Epilimnetic DO generally has lower RMSE than DO in the hypolimnion (Fig. 2). In the epilimnion, RMSE ranges from 0.73 g DO m^{-3} (TR) to 2.11 g DO m^{-3} (ME), and in the hypolimnion, RMSE ranges from 1.20 g DO m^{-3} (TR) to 2.69 g DO m^{-3} (AL). In the southern lakes, modeled values reach anoxic levels and generally follow the DO patterns recorded in the observed data (Fig. 2a-b). Observational data for the northern lakes show an occasional late summer onset of anoxia, and these events are generally captured in the model output. A late summer spike in hypolimnetic DO predictions commonly occurs as well, which is likely a model artifact caused by the reduction of hypolimnetic volumes to very small values over short time periods prior to fall mixing. Reduction to small volumes, coincident with modest fluxes due to high concentration gradients, result in transient high concentrations. Overall, the goodness-of-fit

https://doi.org/10.5194/egusphere-2023-22
Preprint. Discussion started: 11 January 2023

of hypolimnetic DO in our study lakes does not seem to follow any regional or lake characteristic patterns.

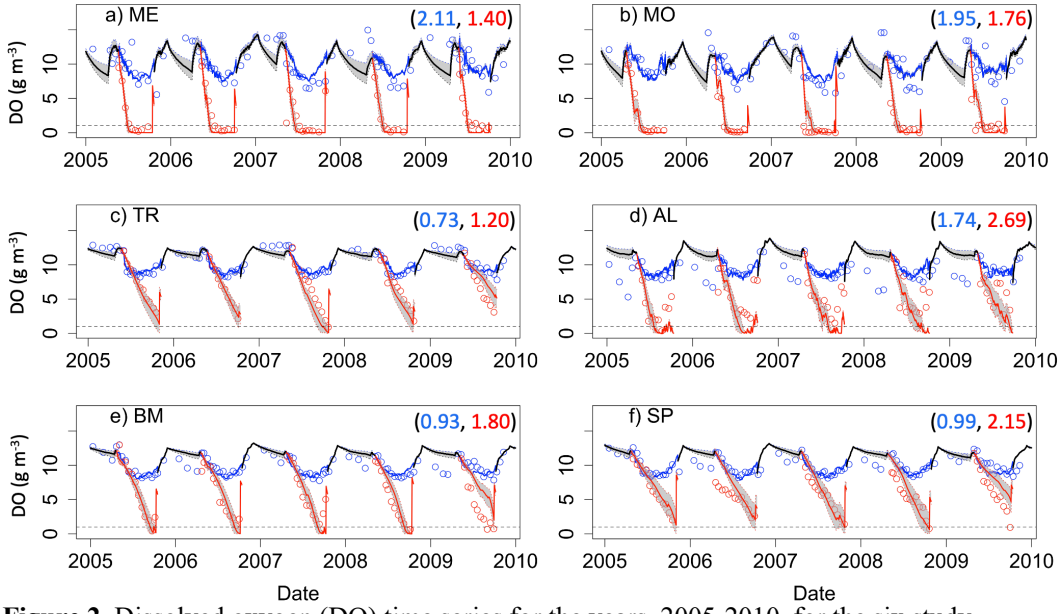

Figure 2. Dissolved oxygen (DO) time series for the years, 2005-2010, for the six study lakes (a-f). Model predictions are represented by lines, and circles represent the observational data. Epilimnetic DO values are blue and Hypolimnetic DO values are red. Fully mixed periods for the lake are indicated by a single black line. RMSE values (epilimnion, hypolimnion; g m^{-3}) are included in the upper right of each panel. Uncertainty is represented by gray shading.

The two southern lakes (ME, MO) have DOC RMSE values equal to or greater than 1.00 g C m^{-3}, while the RMSE for northern lakes ranges from 0.28 g C m^{-3} (TR) to 0.60 g C m^{-3} (AL) (Fig. 3). Observational data in both southern lakes indicate a decrease in DOC concentration beginning around 2010, which is largely missed in the model predictions (Fig.3a-b, Supplementary Material: Fig. S2a-b) and cause an overestimation of DOC by about 1-2 g C m^{-3}. However, model predictions converge with observed DOC toward the end of the study

https://doi.org/10.5194/egusphere-2023-22
Preprint. Discussion started: 11 January 2023

period (Supplementary Material: Fig. S2a-b). In AL, the seasonal patterns of modeled DOC are smaller in amplitude than the observational data (Supplementary Material: Fig. S2d).

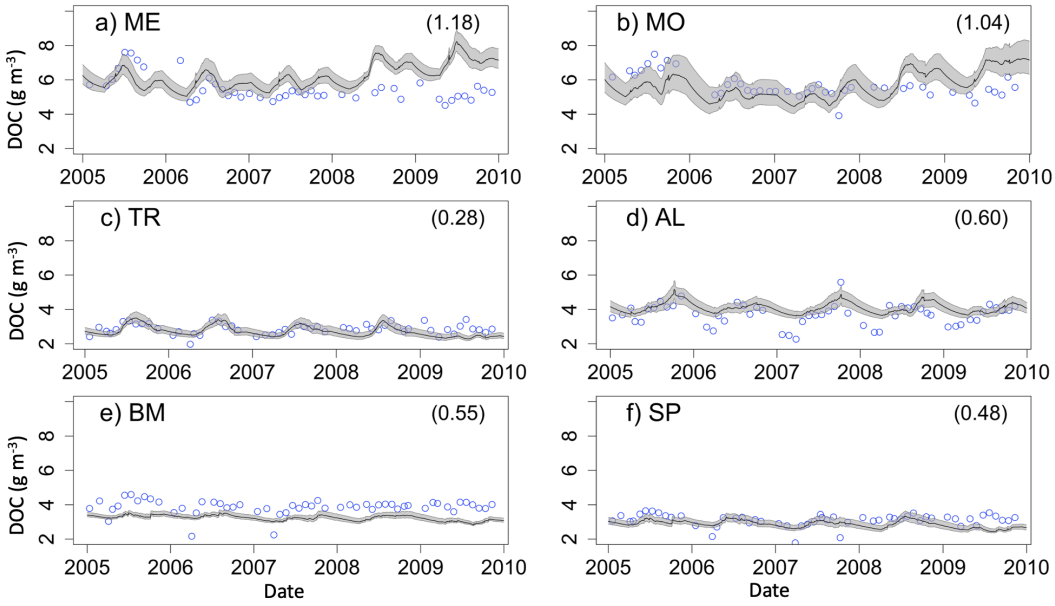

Figure 3. Epilimnetic dissolved organic carbon (DOC) time series for the years, 2005-2010, for the six study lakes (a-f). Model predictions are represented by lines, and circles represent the observational data. RMSE values are included for each lake (g C m^{-3}). Uncertainty is represented by gray shading.

Secchi depth predictions reproduce the mean and seasonal patterns in most lakes (Fig. 4). Although the model produced annual cycles of Secchi depth that generally covered the range of observed values, short term deviations from annual patterns in the observed data are not reproduced. The timing of minima and maxima Secchi depth sometimes differed between predicted and observed values for the northern lakes. In addition, winter extremes in observed Secchi depth are not always reproduced by the model, which is especially evident for ME (Fig. 4a). However, winter observational data for Secchi are more sparse than other seasons.

https://doi.org/10.5194/egusphere-2023-22
Preprint. Discussion started: 11 January 2023

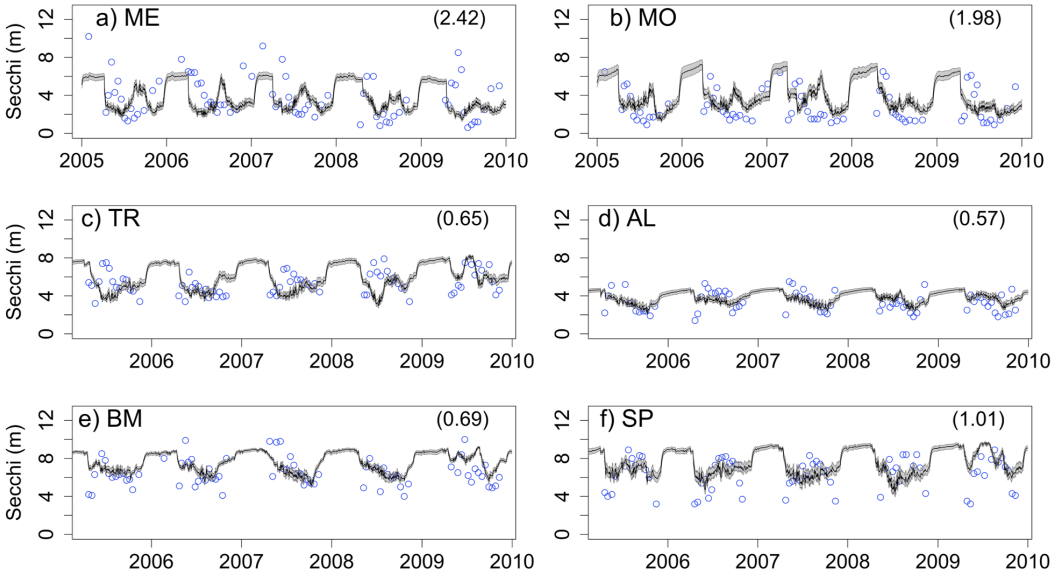

Figure 4. Secchi depth time series for the years, 2005-2010, for the six study lakes (a-f). Model predictions are represented by lines, and circles represent the observational data. RMSE values are included for each lake (m). Uncertainty is represented by gray shading.

3.2 Ecosystem Processes

The mean annual OC budgets of all six lakes show large differences in the sources and fates of OC among lakes (Fig. 5; Supplementary Material: Table S3). Autochthony is the dominant source of OC for all study lakes. Water column respiration is the largest portion of whole-lake respiration in ME, MO, TR, SP, and BM. Sediment respiration contributions are a lower proportion of total respiration in ME, MO, and TR (mean of 15.0%), and are slightly higher in BM and SP (mean of 23.7%). AL has a more even distribution of OC fates. OC burial amounts also vary across the study lakes, with the highest percentage in AL (26.4%), and lowest in SP (2.5%).

https://doi.org/10.5194/egusphere-2023-22
Preprint. Discussion started: 11 January 2023

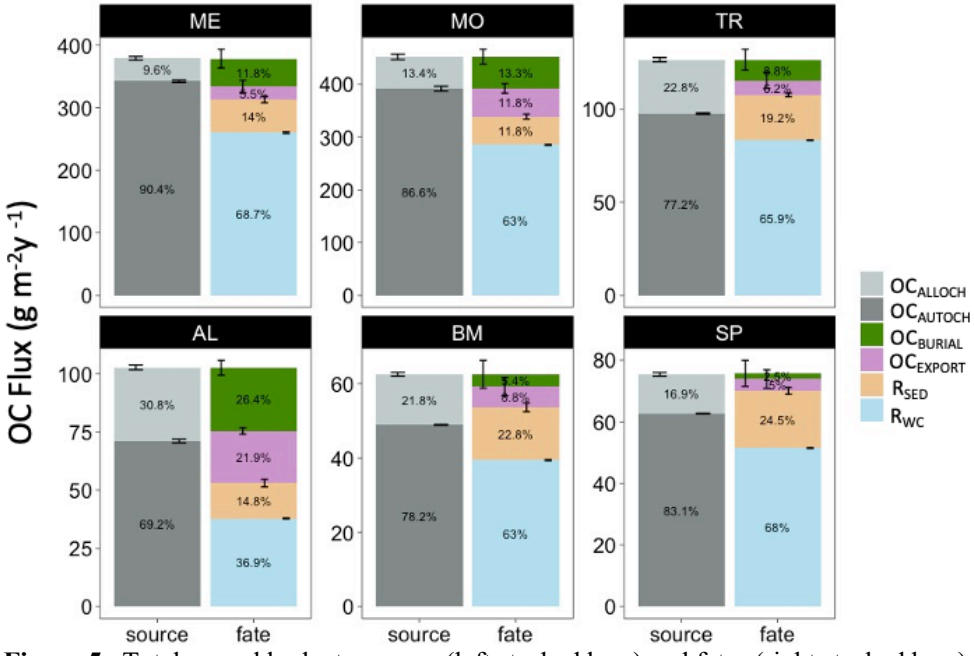

Figure 5. Total annual budget, sources (left stacked bars) and fates (right stacked bars), of organic carbon (OC) in each lake over the study period. The OC sources include allochthonous OC (OC_{ALLOCH}) and autochthonous OC (OC_{AUTOCH}). The OC fates include burial of OC (OC_{BURIAL}), export of OC (OC_{EXPORT}), sediment respiration of OC (R_{SED}), and water column respiration of OC (R_{WC}). Standard error bars for the annual means are indicated for each source and fate as well. Note that the magnitudes of the y-axis differ among the lakes.

The study lakes show inter-annual variation in trophic state, as quantified by NEP (Fig. 6). Total respiration (water column and sediment) exceeds autochthony in SP, BM, and TR, indicating net heterotrophy for these systems. The remaining lakes (ME, MO, AL) are net autotrophic. The southern lakes (ME, MO) were net autotrophic (positive NEP) for the majority of the study years but became less autotrophic over the last five years of the study period (2010-2014). TR, BM, and SP were mostly net heterotrophic (negative NEP) over the

https://doi.org/10.5194/egusphere-2023-22
Preprint. Discussion started: 11 January 2023

study period with a few brief instances of net autotrophy. The strongest autotrophic signal for these lakes occurred around 2010. AL is mostly net autotrophic over the study period but had lower average NEP than the southern lakes. AL also experienced a negative NEP in 2012. ME, MO, and AL all have negative trends in NPP, but only ME was significant (p_value < 0.1, Mann-Kendall test) (SI Table 2). Of these three lakes, ME and AL also have decreasing significant trends in annual total phosphorus concentration (SI Table 2). No significant trends were found for NPP or total phosphorus in the other lakes (MO, TR, BM, SP).

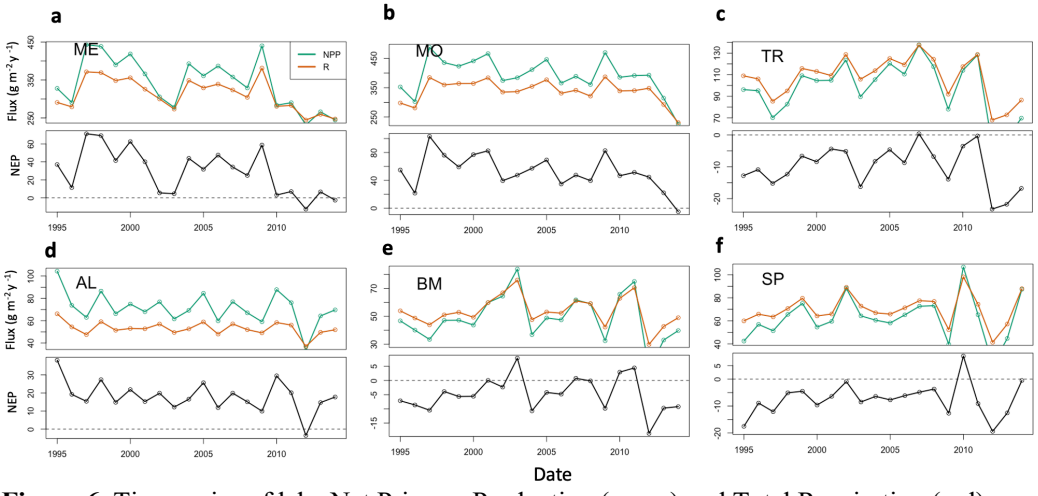

Figure 6. Time series of lake Net Primary Production (green) and Total Respiration (red) (top panels), and Net Ecosystem Production (NEP, bottom panels) for the six lakes: (a) Lake Mendota; (b) Lake Monona; (c) Trout Lake; (d) Allequash Lake; (e) Big Muskellunge Lake, and; (f) Sparkling Lake. Fluxes are in units of $gC\ m^{-2}y^{-1}$

Hypolimnetic DO consumption during stratified periods was due to the two components of hypolimnetic respiration, hypolimnetic water column respiration and hypolimnetic sediment respiration. Water column respiration contributes more than sediment respiration to total hypolimnetic respiration in the southern lakes compared to the northern lakes, with the exception of TR, where cumulative water column respiration is much larger than cumulative

https://doi.org/10.5194/egusphere-2023-22
Preprint. Discussion started: 11 January 2023

sediment respiration. In ME and MO, the mass of summer autochthonous POC entering the hypolimnion is similar to the total hypolimnetic OC mass respired for the beginning of the stratified period (Fig. 7a-b; green line). Later in the stratified period, an increase in epilimnetic POC and associated settling exceeds total hypolimnetic respiration (Fig. 7a-b; green hashed area). This is due, in part, to lower respiration rates that occur once DO (gray line) has been fully depleted, which occurs in early July for ME and late June for MO. In TR and SP the total hypolimnetic respiration slightly exceeds autochthonous POC inputs over the duration of the stratified period, indicating the importance of allochthony in these systems (Fig. 7c,f). BM shows that autochthonous POC entering the hypolimnion and total hypolimnetic respiration are similar throughout the stratified period (Fig. 7d). AL is the only lake to have autochthonous POC inputs consistently larger than total hypolimnetic respiration during the stratified season. All lakes show that summer allochthonous POC entering the hypolimnion is a small contribution to the overall hypolimnetic POC load.

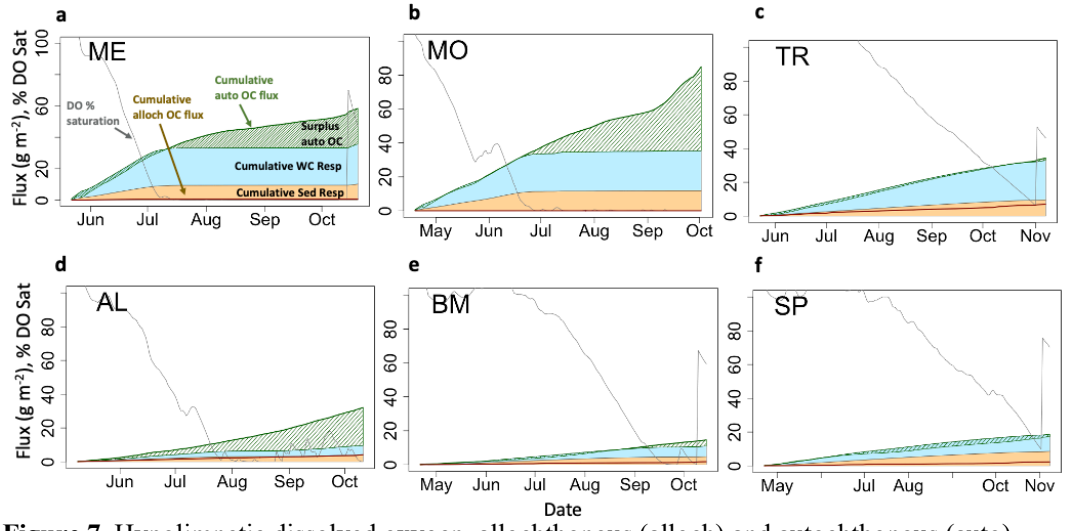

Figure 7. Hypolimnetic dissolved oxygen, allochthonous (alloch) and autochthonous (auto) organic carbon loading, and respiration dynamics during one stratified period (2005) for each

https://doi.org/10.5194/egusphere-2023-22
Preprint. Discussion started: 11 January 2023

lake. Fluxes are cumulative $gC\ m^{-2}$ and DO is presented as percent saturation. Labels are in panel (a). Note that the cumulative water column (WC) and sediment (Sed) respiration fluxes are stacked, while other cumulative fluxes are not.

Respiration of autochthonous POC and sediment respiration account for most of the total hypolimnetic respiration in all lakes (Fig. 8). Respiration of DOC accounts for a relatively small proportion of total respiration. Total hypolimnetic respiration is higher in the southern lakes than the northern lakes. TR has the highest amount of hypolimnetic respiration for the northern lakes, and AL and BM have the least amounts of hypolimnetic respiration. Water column respiration contributed the most towards total hypolimnetic respiration in ME, MO, and TR. Sediment respiration and water column respiration contributed similar proportions towards total hypolimnetic respiration in BM, SP, and AL. As total respiration across lakes increases, a larger proportion of that respiration is attributable to respiration of POC in the water column. DOC water column respiration was the smallest proportion of total hypolimnetic respiration in all six study lakes.

https://doi.org/10.5194/egusphere-2023-22
Preprint. Discussion started: 11 January 2023

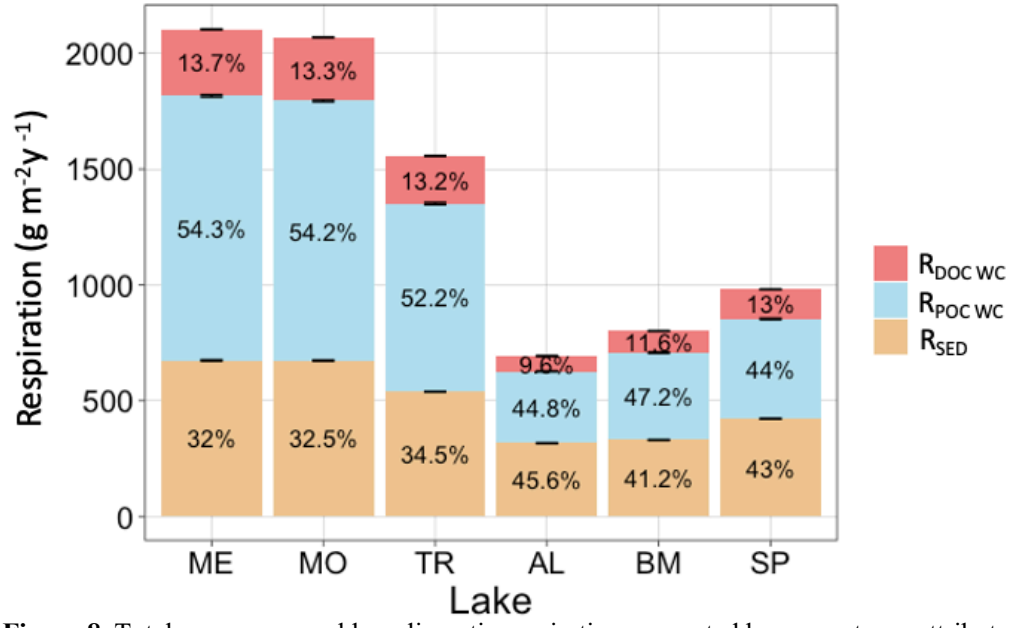

Figure 8. Total average annual hypolimnetic respiration, separated by percentages attributed to water column DOC ($R_{DOC\ WC}$), water column POC ($R_{POC\ WC}$), and sediment (R_{SED}) organic carbon sources. Standard error bars for the annual respiration values are indicated as well.

4 Discussion

4.1 Autochthonous and Allochthonous Loads

Autochthony was the dominant source of OC subsidizing hypolimnetic respiration in the study lakes. The importance of autochthonous OC pools in ecosystem respiration was surprising, given ample research highlighting the dominance of allochthonous OC in north temperate lakes (Wilkinson et al. 2013; Hanson et al. 2011; Hanson et al. 2014). This outcome emphasizes the utility of process-based models in studying mechanisms that discern

https://doi.org/10.5194/egusphere-2023-22
Preprint. Discussion started: 11 January 2023

the relative contributions of different pools of organic matter to lake metabolism. Autochthonous OC pools have higher turnover rates than allochthonous OC pools (Dordoni et al., 2022) and often are lower in concentration than the more recalcitrant allochthonous pools (Wilkinson et al. 2013). Thus, studies based on correlative relationships between lake concentrations of organic matter and water quality metrics, likely overlook the importance of more labile organic matter in driving observable ecosystem phenomena, such as gas flux and formation of hypolimnetic anoxia (Evans et al., 2005; Feng et al., 2022). By quantifying metabolism fluxes relevant to both OC pools, we can recreate shorter-term OC processes that quantify high turnover of labile organic matter, which would typically be missed by empirical studies based on monthly or annual observations.

Allochthony and autochthony are important to lake carbon cycling, but in ways that play out at different time scales. Allochthonous OC has been well-established as an important factor in driving negative NEP through a number of mechanisms (Wilkinson et al., 2013; Hanson et al., 2014; Hanson et al., 2011). Allochthony contributes to water quality variables, such as Secchi depth (Solomon et al. 2015), by providing the bulk of DOC in most lakes (Wilkinson et al., 2013) and can drive persistent hypolimnetic anoxia in dystrophic lakes (Knoll et al., 2018). In contrast, autochthony contributes to seasonal dynamics of water quality through rapid changes in OC that can appear and disappear within a season. Within that seasonal time frame, autochthonous POC settling from the epilimnion can drive hypolimnetic respiration, thus controlling another key water quality metric, oxygen depletion. It is worth noting that our model does not discern allochthonous and autochthonous sediment OC, however we

https://doi.org/10.5194/egusphere-2023-22
Preprint. Discussion started: 11 January 2023

show that autochthonous OC makes up the largest proportion of OC loads in our study lakes and therefore autochthony likely contributes substantially to the sediment OC pool. For highly eutrophic lakes, the model results show excess autochthony stored in the sediments which may carry into subsequent years, potentially providing additional substrate for sediment respiration. Thus, understanding and predicting controls over hypolimnetic oxygen depletion benefits from quantifying both allochthonous and autochthonous OC cycles.

Differences in trophic status, hydrologic residence time, and inflow sources help explain the relative proportion of allochthonous versus autochthonous OC among lakes in our study. Water residence times (Hotchkiss et al. 2018; McCullough et al. 2018) and surrounding land cover (Hanson et al. 2014) have been shown to have a substantial impact on OC dynamics by controlling allochthonous OC loading and NEP trends on lakes included in our study (Hanson et al. 2014, McCullough et al. 2018). We built upon these ideas by recreating daily watershed loading dynamics of POC and DOC from derived discharge data and incorporating nutrient control over lake primary production by using high quality and long-term observational data. The northern lakes are embedded in a forest and wetland landscape, which are characteristic of having higher DOC than the urban and agricultural landscape of the southern lakes (Creed et al., 2003). This creates variation in allochthonous loading across the study lakes. Lake trophic state and productivity are a major control for autochthonous production, which influences autochthonous loads across the study lakes as well. For lake metrics that are comparable between studies, such as allochthonous loading and export,

https://doi.org/10.5194/egusphere-2023-22
Preprint. Discussion started: 11 January 2023

allochthonous water column respiration, and total OC burial, our results were within 20% of values in related studies (Hanson et al. 2014, McCullough et al. 2018).

4.2 Hypolimnetic Respiration

Given the importance of autochthonous POC to hypolimnetic respiration, we assume it contributes substantially to both sediment respiration and respiration in the water column. While previous work found that sediment respiration was the dominant respiration source for lakes with depth ranges encompassed within our study (Steinsberger 2020), we found that water column respiration was at least as important, if not more so. Differences in these findings could be linked to uncertainty in the settling velocity of POC, due to lack of empirical POC settling velocity measurements. Perhaps POC mineralized in the hypolimnia of our modeled lakes passes more quickly to the sediments in real ecosystems, shifting the balance of respiration more toward the sediments. It has been shown that POC respiration contributes substantially to hypolimnetic DO depletion (Jenny et al. 2016), and POC settling velocities can be highly variable, suggesting that assumptions around vertical distribution of lake POC deserve further investigation. Another possible explanation for these differences could be that our model missed allochthonous POC loads from extreme events (Carpenter et al., 2012) which can increase the amount of legacy OC stored in the sediments and increase sediment respiration. Our model also does not account for reduced respiration rates due to OC aging, which may explain our higher values of water column respiration. Finally, our model includes entrainment as a possible oxygen source to the hypolimnion, which must be offset by respiration to fit observed hypolimnetic DO changes. Any study that underestimates

https://doi.org/10.5194/egusphere-2023-22
Preprint. Discussion started: 11 January 2023

DO sources to the hypolimnion likely underestimates total respiration. Our findings highlight the importance of autochthonous POC in hypolimnetic oxygen depletion and suggest that related processes, such as the timing of nutrient loading, changes in thermocline depth, or zooplankton grazing, could impact overall lake respiration dynamics and anoxia formation (Schindler et al., 2016; Ladwig et al., 2021; Müller et al., 2012).

4.3 Long-term Dynamics

Although autochthonous OC dominated the loads across the study lakes, analysis of the long-term OC dynamics supports the importance of allochthony in lakes. Net Ecosystem Production (NEP) has been used to quantify heterotrophy and autotrophy in lakes (Odum 1956, Hanson et al. 2003, Cole et al. 2000, Lovett et al. 2006), and using this metric over multiple decades allowed us to analyze long-term impacts of allochthony. TR, BM, and SP fluctuated between heterotrophy and autotrophy, usually in tandem with trends in hydrology, which acts as a main control of allochthonous OC. This suggests that allochthonous OC inputs may be less important for seasonal anoxia but can still drive a lake toward negative NEP and contribute to sediment carbon storage over long time periods. ME, MO, and AL tended to become less autotrophic over time (Fig. 6), a pattern that coincided with significant decreasing trends in mean epilimnetic total phosphorus concentrations for two of the lakes, ME and AL (SI Fig. 5). In our model NPP and phosphorus are directly related, so decreases in phosphorus are likely to cause decreases in NEP. Short-term respiration of autochthonous POC can account for rapid decreases in hypolimnetic DO, but allochthonous POC, which tends to be more recalcitrant, provides long-term subsidy of ecosystem respiration that can

https://doi.org/10.5194/egusphere-2023-22
Preprint. Discussion started: 11 January 2023

result in long-term net heterotrophy. Thus, it's critical to understand and quantify both the rapid internal cycling based on autochthony and the long and slow turnover of allochthony.

Through a perspective that includes cycling of both allochthony and autochthony, we can expand our conceptual model of metabolism to better understand time dynamics of lake water quality at the ecosystem scale. Autochthony has pronounced seasonal dynamics, typically associated with the temporal variability of phytoplankton communities and the growth and senescence of macrophytes (Rautio et al., 2011). While allochthony can also have strong seasonal patterns associated with leaf litter input, pollen blooms, and spring runoff events, its more recalcitrant nature leads to a less pronounced seasonal signal at the ecosystem scale (Wilkinson et al., 2013, Tranvik 1998). When considered together, it seems that allochthony underlies long and slow changes in metabolism patterns, while autochthony overlays strong seasonality. Both OC pools are important for ecosystem scale metabolism processes, and their consequences are evident at different time scales. Therefore, the interactions of both OC sources and their influences on water quality patterns deserve further investigation.

Autochthonous OC control over hypolimnetic respiration should be a primary consideration for understanding the influence of OC on ecosystem dynamics. Hypolimnetic oxygen depletion and anoxia in productive lakes can be mitigated by reducing autochthonous production of OC, which we show is mainly driven by nutrient availability. This study also identifies the need for a better understanding of internal and external OC loads in lakes.

https://doi.org/10.5194/egusphere-2023-22
Preprint. Discussion started: 11 January 2023

669 Previous studies have found heterotrophic behavior in less productive lakes, but our findings
670 highlight the importance of autochthony in these lakes, especially for shorter-time scale
671 processes that can be missed by looking at broad annual patterns. By using a one-
672 dimensional model, we are able to also understand how surface metabolism processes can
673 impact bottom layer dynamics, which would not be possible with a zero-dimensional model.
674 Looking forward, we believe that our understanding of these processes could be improved by
675 building a coupled watershed - metabolism model to more closely explore causal relations
676 between watershed hydrology, nutrient dynamics, and lake morphometry.
677
678
679

https://doi.org/10.5194/egusphere-2023-22
Preprint. Discussion started: 11 January 2023

Code Availability
Model code and figure creation code are archived in the Environmental Data Initiative repository (https://doi.org/10.6073/PASTA/1B5B947999AA2F9E0E95C91782B36EE9, Delany, 2022).

Data Availability
Driving data, model configuration files, and model result data are archived in the Environmental Data Initiative repository (https://doi.org/10.6073/PASTA/1B5B947999AA2F9E0E95C91782B36EE9, Delany, 2022).

Author Contributions
AD, PH, RL, and CB assisted with model development and analysis of results. AD and PH prepared the manuscript with contributions from RL, CB, and EA.

Competing Interests
The authors declare that they have no conflict of interest.

Acknowledgements:
Funding was provided through the National Science Foundation (NSF), with grants DEB-1753639, DEB-1753657, and DEB-2025982. Funding for Ellen Albright was provided by the NSF Graduate Research Fellowship Program (GRFP), and the Iowa Department of Natural Resources (contract #22CRDLWBMBALM-0002). Funding for Robert Ladwig was provided by the NSF ABI development grant (#DBI 1759865), UW-Madison Data Science Initiative grant, and the NSF HDR grant (#1934633). Data were provided by the North Temperate Lakes Long Term Ecological Research Program and was accessed through the Environmental Data Initiative (DOI: 10.6073/pasta/0dbbfdbcdee623477c000106c444f3fd).

https://doi.org/10.5194/egusphere-2023-22
Preprint. Discussion started: 11 January 2023

References

Bryant, L. D., Hsu-Kim, H., Gantzer, P. A., & Little, J. C. (2011). Solving the problem at the source: Controlling Mn release at the sediment-water interface via hypolimnetic oxygenation. *Water Research*, *45*(19), 6381–6392. https://doi.org/10.1016/j.watres.2011.09.030

Cardille, J. A., Carpenter, S. R., Coe, M. T., Foley, J. A., Hanson, P. C., Turner, M. G., & Vano, J. A. (2007). Carbon and water cycling in lake-rich landscapes: Landscape connections, lake hydrology, and biogeochemistry. *Journal of Geophysical Research*, *112*(G2), G02031. https://doi.org/10.1029/2006JG000200

Carpenter, S., Arrow, K., Barrett, S., Biggs, R., Brock, W., Crépin, A.-S., Engström, G., Folke, C., Hughes, T., Kautsky, N., Li, C.-Z., McCarney, G., Meng, K., Mäler, K.-G., Polasky, S., Scheffer, M., Shogren, J., Sterner, T., Vincent, J., … Zeeuw, A. (2012). General Resilience to Cope with Extreme Events. *Sustainability*, *4*(12), 3248–3259. https://doi.org/10.3390/su4123248

Cole, G., & Weihe, P. (2016). *Textbook of Limnology*. Waveland Press, Inc.

Cole, J. J., & Caraco, N. F. (1998). Atmospheric exchange of carbon dioxide in a low-wind oligotrophic lake measured by the addition of SF_6. *Limnology and Oceanography*, *43*(4), 647–656. https://doi.org/10.4319/lo.1998.43.4.0647

Cole, J. J., Pace, M. L., Carpenter, S. R., & Kitchell, J. F. (2000). Persistence of net heterotrophy in lakes during nutrient addition and food web manipulations. *Limnology and Oceanography*, *45*(8), 1718–1730. https://doi.org/10.4319/lo.2000.45.8.1718

https://doi.org/10.5194/egusphere-2023-22
Preprint. Discussion started: 11 January 2023

728 Creed, I. F., Sanford, S. E., Beall, F. D., Molot, L. A., & Dillon, P. J. (2003). Cryptic
729 wetlands: Integrating hidden wetlands in regression models of the export of dissolved
730 organic carbon from forested landscapes. *Hydrological Processes*, *17*(18), 3629–3648.
731 https://doi.org/10.1002/hyp.1357
732 Delany, A. (2022). *Modeled Organic Carbon, Dissolved Oxygen, and Secchi for six*
733 *Wisconsin Lakes, 1995-2014* [Data set]. Environmental Data Initiative.
734 https://doi.org/10.6073/PASTA/1B5B947999AA2F9E0E95C91782B36EE9
735 Dordoni, M., Seewald, M., Rinke, K., van Geldern, R., Schmidmeier, J., & Barth, J. A. C.
736 (2022). *Mineralization of autochthonous particulate organic carbon is a fast channel of*
737 *organic matter turnover in Germany's largest drinking water reservoir* [Preprint].
738 Biogeochemistry: Stable Isotopes & Other Tracers. https://doi.org/10.5194/bg-
739 2022-154
740 Evans, C. D., Monteith, D. T., & Cooper, D. M. (2005). Long-term increases in surface water
741 dissolved organic carbon: Observations, possible causes and environmental impacts.
742 *Environmental Pollution*, *137*(1), 55–71. https://doi.org/10.1016/j.envpol.2004.12.031
743 Feng, L., Zhang, J., Fan, J., Wei, L., He, S., & Wu, H. (2022). Tracing dissolved organic
744 matter in inflowing rivers of Nansi Lake as a storage reservoir: Implications for water-
745 quality control. *Chemosphere*, *286*, 131624.
746 https://doi.org/10.1016/j.chemosphere.2021.131624
747 Hanson, P. C., Bade, D. L., Carpenter, S. R., & Kratz, T. K. (2003). Lake metabolism:
748 Relationships with dissolved organic carbon and phosphorus. *Limnology and*
749 *Oceanography*, *48*(3), 1112–1119. https://doi.org/10.4319/lo.2003.48.3.1112

https://doi.org/10.5194/egusphere-2023-22
Preprint. Discussion started: 11 January 2023

Hanson, P. C., Buffam, I., Rusak, J. A., Stanley, E. H., & Watras, C. (2014). Quantifying lake allochthonous organic carbon budgets using a simple equilibrium model. *Limnology and Oceanography*, *59*(1), 167–181. https://doi.org/10.4319/lo.2014.59.1.0167

Hanson, P. C., Hamilton, D. P., Stanley, E. H., Preston, N., Langman, O. C., & Kara, E. L. (2011). Fate of Allochthonous Dissolved Organic Carbon in Lakes: A Quantitative Approach. *PLoS ONE*, *6*(7), e21884. https://doi.org/10.1371/journal.pone.0021884

Hanson, P. C., Pace, M. L., Carpenter, S. R., Cole, J. J., & Stanley, E. H. (2015). Integrating Landscape Carbon Cycling: Research Needs for Resolving Organic Carbon Budgets of Lakes. *Ecosystems*, *18*(3), 363–375. https://doi.org/10.1007/s10021-014-9826-9

Hanson, P. C., Pollard, A. I., Bade, D. L., Predick, K., Carpenter, S. R., & Foley, J. A. (2004). A model of carbon evasion and sedimentation in temperate lakes: LANDSCAPE-LAKE CARBON CYCLING MODEL. *Global Change Biology*, *10*(8), 1285–1298. https://doi.org/10.1111/j.1529-8817.2003.00805.x

Hanson, P. C., Stillman, A. B., Jia, X., Karpatne, A., Dugan, H. A., Carey, C. C., Stachelek, J., Ward, N. K., Zhang, Y., Read, J. S., & Kumar, V. (2020). Predicting lake surface water phosphorus dynamics using process-guided machine learning. *Ecological Modelling*, *430*, 109136. https://doi.org/10.1016/j.ecolmodel.2020.109136

Hart, J., Dugan, H., Carey, C., Stanley, E., & Hanson, P. (2019). *Lake Mendota Carbon and Greenhouse Gas Measurements at North Temperate Lakes LTER 2016* [Data set]. Environmental Data Initiative. https://doi.org/10.6073/PASTA/170E5BA0ED09FE3D5837EF04C47E432E

https://doi.org/10.5194/egusphere-2023-22
Preprint. Discussion started: 11 January 2023

771 Hipsey, M. R., Bruce, L. C., Boon, C., Busch, B., Carey, C. C., Hamilton, D. P., Hanson, P.
772 C., Read, J. S., de Sousa, E., Weber, M., & Winslow, L. A. (2019). A General Lake
773 Model (GLM 3.0) for linking with high-frequency sensor data from the Global Lake
774 Ecological Observatory Network (GLEON). *Geoscientific Model Development*, *12*(1),
775 473–523. https://doi.org/10.5194/gmd-12-473-2019
776 Hoffman, A. R., Armstrong, D. E., & Lathrop, R. C. (2013). Influence of phosphorus
777 scavenging by iron in contrasting dimictic lakes. *Canadian Journal of Fisheries and*
778 *Aquatic Sciences*, *70*(7), 941–952. https://doi.org/10.1139/cjfas-2012-0391
779 Hotchkiss, E. R., Sadro, S., & Hanson, P. C. (2018). Toward a more integrative perspective
780 on carbon metabolism across lentic and lotic inland waters. *Limnology and*
781 *Oceanography Letters*, *3*(3), 57–63. https://doi.org/10.1002/lol2.10081
782 Hunt, R. J., & Walker, J. F. (2017). *2016 Update to the GSFLOW groundwater-surface water*
783 *model for the Trout Lake Watershed*. https://doi.org/10.5066/F7M32SZ2
784 Hunt, R. J., Walker, J. F., Selbig, W. R., Westenbroek, S. M., & Regan, R. S. (2013).
785 *Simulation of Climate-Change Effects on Streamflow, Lake Water Budgets, and Stream*
786 *Temperature Using GSFLOW and SNTEMP, Trout Lake Watershed, Wisconsin*. United
787 States Geological Survey.
788 Jane, S. F., Hansen, G. J. A., Kraemer, B. M., Leavitt, P. R., Mincer, J. L., North, R. L., Pilla,
789 R. M., Stetler, J. T., Williamson, C. E., Woolway, R. I., Arvola, L., Chandra, S.,
790 DeGasperi, C. L., Diemer, L., Dunalska, J., Erina, O., Flaim, G., Grossart, H.-P.,
791 Hambright, K. D., … Rose, K. C. (2021). Widespread deoxygenation of temperate lakes.
792 *Nature*, *594*(7861), 66–70. https://doi.org/10.1038/s41586-021-03550-y

https://doi.org/10.5194/egusphere-2023-22
Preprint. Discussion started: 11 January 2023

793 Jenny, J.-P., Francus, P., Normandeau, A., Lapointe, F., Perga, M.-E., Ojala, A.,
794 Schimmelmann, A., & Zolitschka, B. (2016). Global spread of hypoxia in freshwater
795 ecosystems during the last three centuries is caused by rising local human pressure.
796 *Global Change Biology*, *22*(4), 1481–1489. https://doi.org/10.1111/gcb.13193
797 Jenny, J.-P., Normandeau, A., Francus, P., Taranu, Z. E., Gregory-Eaves, I., Lapointe, F.,
798 Jautzy, J., Ojala, A. E. K., Dorioz, J.-M., Schimmelmann, A., & Zolitschka, B. (2016).
799 Urban point sources of nutrients were the leading cause for the historical spread of
800 hypoxia across European lakes. *Proceedings of the National Academy of Sciences*,
801 *113*(45), 12655–12660. https://doi.org/10.1073/pnas.1605480113
802 Knoll, L. B., Williamson, C. E., Pilla, R. M., Leach, T. H., Brentrup, J. A., & Fisher, T. J.
803 (2018). Browning-related oxygen depletion in an oligotrophic lake. *Inland Waters*, *8*(3),
804 255–263. https://doi.org/10.1080/20442041.2018.1452355
805 Kraemer, B. M., Chandra, S., Dell, A. I., Dix, M., Kuusisto, E., Livingstone, D. M.,
806 Schladow, S. G., Silow, E., Sitoki, L. M., Tamatamah, R., & McIntyre, P. B. (2017).
807 Global patterns in lake ecosystem responses to warming based on the temperature
808 dependence of metabolism. *Global Change Biology*, *23*(5), 1881–1890.
809 https://doi.org/10.1111/gcb.13459
810 Ladwig, R., Hanson, P. C., Dugan, H. A., Carey, C. C., Zhang, Y., Shu, L., Duffy, C. J., &
811 Cobourn, K. M. (2021). Lake thermal structure drives interannual variability in summer
812 anoxia dynamics in a eutrophic lake over 37 years. *Hydrology and Earth System*
813 *Sciences*, *25*(2), 1009–1032. https://doi.org/10.5194/hess-25-1009-2021

https://doi.org/10.5194/egusphere-2023-22
Preprint. Discussion started: 11 January 2023

814 Lathrop, R., & Carpenter, S. (2014). Water quality implications from three decades of
815 phosphorus loads and trophic dynamics in the Yahara chain of lakes. *Inland Waters*,
816 *4*(1), 1–14. https://doi.org/10.5268/IW-4.1.680
817 Lei, R., Leppäranta, M., Erm, A., Jaatinen, E., & Pärn, O. (2011). Field investigations of
818 apparent optical properties of ice cover in Finnish and Estonian lakes in winter 2009.
819 *Estonian Journal of Earth Sciences*, *60*(1), 50. https://doi.org/10.3176/earth.2011.1.05
820 Livingstone, D. M., & Imboden, D. M. (1996). The prediction of hypolimnetic oxygen
821 profiles: A plea for a deductive approach. *Canadian Journal of Fisheries and Aquatic*
822 *Sciences*, *53*(4), 924–932. https://doi.org/10.1139/f95-230
823 Loose, B., & Schlosser, P. (2011). Sea ice and its effect on CO_2 flux between the atmosphere
824 and the Southern Ocean interior. *Journal of Geophysical Research: Oceans*, *116*(C11),
825 2010JC006509. https://doi.org/10.1029/2010JC006509
826 Lovett, G. M., Cole, J. J., & Pace, M. L. (2006). Is Net Ecosystem Production Equal to
827 Ecosystem Carbon Accumulation? *Ecosystems*, *9*(1), 152–155.
828 https://doi.org/10.1007/s10021-005-0036-3
829 Magee, M. R., McIntyre, P. B., Hanson, P. C., & Wu, C. H. (2019). Drivers and Management
830 Implications of Long-Term Cisco Oxythermal Habitat Decline in Lake Mendota, WI.
831 *Environmental Management*, *63*(3), 396–407. https://doi.org/10.1007/s00267-018-
832 01134-7
833 Magnuson, J., Carpenter, S., & Stanley, E. (2020). *North Temperate Lakes LTER: Chemical*
834 *Limnology of Primary Study Lakes: Nutrients, pH and Carbon 1981 - current* [Data set].

https://doi.org/10.5194/egusphere-2023-22
Preprint. Discussion started: 11 January 2023

Environmental Data Initiative. https://doi.org/10.6073/PASTA/8359D27BBD91028F222D923A7936077D

Magnuson, J. J., Benson, B. J., & Kratz, T. K. (2006). *Long-term dynamics of lakes in the landscape: Long-term ecological research on north temperate lakes.* Oxford University Press on Demand.

Magnuson, J. J., Carpenter, S. R., & Stanley, E. H. (2022). *North Temperate Lakes LTER: Physical Limnology of Primary Study Lakes 1981 - current* [Data set]. Environmental Data Initiative. https://doi.org/10.6073/PASTA/925D94173F35471F699B5BC343AA1128

McClure, R. P., Lofton, M. E., Chen, S., Krueger, K. M., Little, J. C., & Carey, C. C. (2020). The Magnitude and Drivers of Methane Ebullition and Diffusion Vary on a Longitudinal Gradient in a Small Freshwater Reservoir. *Journal of Geophysical Research: Biogeosciences*, *125*(3). https://doi.org/10.1029/2019JG005205

McCullough, I. M., Dugan, H. A., Farrell, K. J., Morales-Williams, A. M., Ouyang, Z., Roberts, D., Scordo, F., Bartlett, S. L., Burke, S. M., Doubek, J. P., Krivak-Tetley, F. E., Skaff, N. K., Summers, J. C., Weathers, K. C., & Hanson, P. C. (2018). Dynamic modeling of organic carbon fates in lake ecosystems. *Ecological Modelling*, *386*, 71–82. https://doi.org/10.1016/j.ecolmodel.2018.08.009

Müller, B., Bryant, L. D., Matzinger, A., & Wüest, A. (2012). Hypolimnetic Oxygen Depletion in Eutrophic Lakes. *Environmental Science & Technology*, *46*(18), 9964–9971. https://doi.org/10.1021/es301422r

https://doi.org/10.5194/egusphere-2023-22
Preprint. Discussion started: 11 January 2023

856 Nürnberg, G. K. (1995). Quantifying anoxia in lakes. *Limnology and Oceanography*, *40*(6),
857 1100–1111. https://doi.org/10.4319/lo.1995.40.6.1100
858 Nürnberg, G. K. (2004). Quantified Hypoxia and Anoxia in Lakes and Reservoirs. *The*
859 *Scientific World JOURNAL*, *4*, 42–54. https://doi.org/10.1100/tsw.2004.5
860 Odum, H. T. (1956). Primary Production in Flowing Waters. *Limnology and Oceanography*,
861 *1*(2), 102–117. https://doi.org/10.4319/lo.1956.1.2.0102
862 Platt, T., Gallegos, C., & Harrison, W. (1980). Photoinhibition of photosynthesis in natural
863 assemblages of marine phytoplankton. *Journal of Marine Research*, *38*(4), 687–701.
864 Qu, Y., & Duffy, C. J. (2007). A semidiscrete finite volume formulation for multiprocess
865 watershed simulation: MULTIPROCESS WATERSHED SIMULATION. *Water*
866 *Resources Research*, *43*(8). https://doi.org/10.1029/2006WR005752
867 Rautio, M., Mariash, H., & Forsström, L. (2011). Seasonal shifts between autochthonous and
868 allochthonous carbon contributions to zooplankton diets in a subarctic lake. *Limnology*
869 *and Oceanography*, *56*(4), 1513–1524. https://doi.org/10.4319/lo.2011.56.4.1513
870 Read, J. S., Hamilton, D. P., Jones, I. D., Muraoka, K., Winslow, L. A., Kroiss, R., Wu, C.
871 H., & Gaiser, E. (2011). Derivation of lake mixing and stratification indices from high-
872 resolution lake buoy data. *Environmental Modelling & Software*, *26*(11), 1325–1336.
873 https://doi.org/10.1016/j.envsoft.2011.05.006
874 Read, J. S., Zwart, J. A., Kundel, H., Corson-Dosch, H. R., Hansen, G. J. A., Vitense, K.,
875 Appling, A. P., Oliver, S. K., & Platt, L. (2021). *Data release: Process-based*
876 *predictions of lake water temperature in the Midwest US* [Data set]. U.S. Geological
877 Survey. https://doi.org/10.5066/P9CA6XP8

https://doi.org/10.5194/egusphere-2023-22
Preprint. Discussion started: 11 January 2023

878 Reynolds, C. S., Oliver, R. L., & Walsby, A. E. (1987). Cyanobacterial dominance: The role
879 of buoyancy regulation in dynamic lake environments. *New Zealand Journal of Marine*
880 *and Freshwater Research*, *21*(3), 379–390.
881 https://doi.org/10.1080/00288330.1987.9516234
882 Rhodes, J., Hetzenauer, H., Frassl, M. A., Rothhaupt, K.-O., & Rinke, K. (2017). Long-term
883 development of hypolimnetic oxygen depletion rates in the large Lake Constance.
884 *Ambio*, *46*(5), 554–565. https://doi.org/10.1007/s13280-017-0896-8
885 Richardson, D. C., Carey, C. C., Bruesewitz, D. A., & Weathers, K. C. (2017). Intra- and
886 inter-annual variability in metabolism in an oligotrophic lake. *Aquatic Sciences*, *79*(2),
887 319–333. https://doi.org/10.1007/s00027-016-0499-7
888 Rippey, B., & McSorley, C. (2009). Oxygen depletion in lake hypolimnia. *Limnology and*
889 *Oceanography*, *54*(3), 905–916. https://doi.org/10.4319/lo.2009.54.3.0905
890 Schindler, D. W., Carpenter, S. R., Chapra, S. C., Hecky, R. E., & Orihel, D. M. (2016).
891 Reducing Phosphorus to Curb Lake Eutrophication is a Success. *Environmental Science*
892 *& Technology*, *50*(17), 8923–8929. https://doi.org/10.1021/acs.est.6b02204
893 Snortheim, C. A., Hanson, P. C., McMahon, K. D., Read, J. S., Carey, C. C., & Dugan, H. A.
894 (2017). Meteorological drivers of hypolimnetic anoxia in a eutrophic, north temperate
895 lake. *Ecological Modelling*, *343*, 39–53.
896 https://doi.org/10.1016/j.ecolmodel.2016.10.014
897 Solomon, C. T., Jones, S. E., Weidel, B. C., Buffam, I., Fork, M. L., Karlsson, J., Larsen, S.,
898 Lennon, J. T., Read, J. S., Sadro, S., & Saros, J. E. (2015). Ecosystem Consequences of
899 Changing Inputs of Terrestrial Dissolved Organic Matter to Lakes: Current Knowledge

https://doi.org/10.5194/egusphere-2023-22
Preprint. Discussion started: 11 January 2023

and Future Challenges. *Ecosystems*, *18*(3), 376–389. https://doi.org/10.1007/s10021-015-9848-y

Staehr, P. A., Bade, D., Van de Bogert, M. C., Koch, G. R., Williamson, C., Hanson, P., Cole, J. J., & Kratz, T. (2010). Lake metabolism and the diel oxygen technique: State of the science: Guideline for lake metabolism studies. *Limnology and Oceanography: Methods*, *8*(11), 628–644. https://doi.org/10.4319/lom.2010.8.0628

Steinsberger, T., Schwefel, R., Wüest, A., & Müller, B. (2020). Hypolimnetic oxygen depletion rates in deep lakes: Effects of trophic state and organic matter accumulation. *Limnology and Oceanography*, *65*(12), 3128–3138. https://doi.org/10.1002/lno.11578

Thorp, J. H., & Delong, M. D. (2002). Dominance of autochthonous autotrophic carbon in food webs of heterotrophic rivers. *Oikos*, *96*(3), 543–550. https://doi.org/10.1034/j.1600-0706.2002.960315.x

Tranvik, L. J. (1998). Degradation of Dissolved Organic Matter in Humic Waters by Bacteria. In D. O. Hessen & L. J. Tranvik (Eds.), *Aquatic Humic Substances* (Vol. 133, pp. 259–283). Springer Berlin Heidelberg. https://doi.org/10.1007/978-3-662-03736-2_11

Webster, K. E., Kratz, T. K., Bowser, C. J., Magnuson, J. J., & Rose, W. J. (1996). The influence of landscape position on lake chemical responses to drought in northern Wisconsin. *Limnology and Oceanography*, *41*(5), 977–984. https://doi.org/10.4319/lo.1996.41.5.0977

https://doi.org/10.5194/egusphere-2023-22
Preprint. Discussion started: 11 January 2023

Wilkinson, G. M., Pace, M. L., & Cole, J. J. (2013). Terrestrial dominance of organic matter in north temperate lakes: ORGANIC MATTER COMPOSITION IN LAKES. *Global Biogeochemical Cycles*, *27*(1), 43–51. https://doi.org/10.1029/2012GB004453

Williamson, C. E., Dodds, W., Kratz, T. K., & Palmer, M. A. (2008). Lakes and streams as sentinels of environmental change in terrestrial and atmospheric processes. *Frontiers in Ecology and the Environment*, *6*(5), 247–254. https://doi.org/10.1890/070140

Winslow, L. A., Zwart, J. A., Batt, R. D., Dugan, H. A., Woolway, R. I., Corman, J. R., Hanson, P. C., & Read, J. S. (2016). LakeMetabolizer: An R package for estimating lake metabolism from free-water oxygen using diverse statistical models. *Inland Waters*, *6*(4), 622–636. https://doi.org/10.1080/IW-6.4.883